

Guijun Xian\*, Hui Li

## 4 Hygrothermal Aging of an Ultraviolet Cured Glass-fiber Reinforced Acrylate Composite

**Abstract:** Ultraviolet (UV) cured glass fiber reinforced acrylate polymer (GFRP) composites can be fully cured in several ten seconds with assistance of a UV lamp, which could potentially be used for quick repair of concrete structures. Besides the basic mechanical properties (e.g., tensile properties, bonding to concrete substrates), the degradation of the UV-GFRP subjected to water or concrete pore solution (strong alkaline with pH value around 13) immersion with or without an external sustained bending deformation is concerned in application. In this chapter, the hygrothermal aging of UV cured GFRP composites subjected to water or alkaline solution immersion is demonstrated in terms of water uptake, mechanical properties and glass transition temperatures. The effects of sustained bending on the degradation of the UV-GFRP samples are also presented.

**Keywords:** Fiber Reinforced Polymer; Environmental degradation; Durability

### 4.1 Introduction

In recent years, fiber reinforced polymer (FRP) composites have been widely accepted for rehabilitation, strengthening and upgrading infrastructures through external bonding technology (Hollaway, 2009; Jumaat et al., 2010; Karbhari and Abanilla, 2007; Pendhari et al., 2008). Compared to the traditional civil engineering materials (i.e., steel and concrete), FRP composites possess many irreplaceable advantages in terms of light weight, high strength, excellent corrosive resistance, ease of installation, etc. (Bank et al., 2007).

The FRPs used in this field mainly include carbon, glass and Aramide fibers reinforced wet lay-ups, prepregs and pre-cured strips. Among them, fiber fabric reinforced ambient curable resin based wet lay-ups are dominant due to low cost, ease of installation and improved bonding strength to the concrete substrate. The curing

---

\*Corresponding author: **Guijun Xian**, Key Lab of Structures Dynamic Behavior and Control (Harbin Institute of Technology), Ministry of Education, Heilongjiang, Harbin, 150090, China,  
E-Mail: gjxian@hit.edu.cn / xianguijun@163.com

**Hui Li**, Key Lab of Structures Dynamic Behavior and Control (Harbin Institute of Technology), Ministry of Education, Heilongjiang, Harbin, 150090, China

**Guijun Xian, Hui Li**, School of Civil Engineering, Harbin Institute of Technology, Heilongjiang, Harbin, 150090, China

of wet lay-ups with ambient curable resins at room temperature is a time consuming process, and generally, several days of curing is required to reach necessary mechanical properties (Li and Ghebreyesus, 2006). The required long curing time undoubtedly creates many problems, especially when those FRPs are used to repair bridges, roads and some key infrastructures. For example, the delayed opening to traffic of a bridge in repair will result in a significant economic cost. In addition, while during some emergent situations, e.g., in earthquake, the quick recovery of the traffic is more crucial for saving lives.

Ultraviolet (UV) light curing technology can cure some kinds of resins in a very fast rate, exhibiting a high potential to quickly cure the FRPs (Compston et al., 2008; Di Pietro and Compston, 2009; Duan et al., 2011), and so help the prompt repair of concrete structures. Presently, UV curing technology has already been accepted by the coating and ink industries. UV curable resin systems can be fully cured by exposure to UV sources in a much shorter time (e.g., just over a minute), and do not have “gel time” that is one of important characteristics of a conventional resin system. Due to the existence of gel time, the processing time should be controlled precisely for conventional resins (e.g., epoxy). Without “gel time”, however, the processing time is flexible for the UV curing system, which will benefit quality control and reduce waste of raw materials. In addition, due to the fast curing of UV systems, the emissions of volatile organic compounds (VOCs) can be dramatically reduced (Compston et al., 2008). Therefore, the UV curing technology is also considered environmental friendly in contrast to the conventional resins.

With UV curing technology, UV curable fiber reinforced polymer (FRP) composites can be expected to be cured in seconds, and thus “fast repair” of infrastructures may be realized. It is worth noting that UV curing FRP systems have been ever used in repair of composite structures (Peck et al., 2007). Meanwhile, until now, attempts have been made to use the UV curing technology to repair damaged concrete structures (Li and Ghebreyesus, 2006; Li et al., 2003). In one precursory exploitation on UV curing FRP composites in the repair of damaged reinforced concrete columns, the UV curing FRPs were shown to be fast, strong, durable (in seawater) and cost effective, as compared to conventional ambient curing epoxy resin based wet lay-ups (Li and Ghebreyesus, 2006).

Since the FRP strengthened structures are generally expected to work more than 50 years, the durability of the FRPs in harsh environments is crucial for their acceptance and design in rehabilitation (Karbhari and Xian, 2009). The long term durability of FRPs in harsh civil engineering environments, however, is not yet well understood, which adversely affects their safe, economic and wide application (Karbhari et al., 2003). During the service life of a FRP composite, water uptake and diffusion are inevitable, which will bring in plasticization, swelling, hydrolysis of polymer matrix, debonding of fibers from the resin, as well as the corrosion of fibers (glass or Aramid fibers) (Xian and Karbhari, 2007a; Xian and Karbhari, 2007b). As a result, the mechanical and thermal properties degrade, and the service life is

shortened accordingly. Because the concrete pore solution is a strong alkaline (pH value about 13), the durability of FRPs exposed to a strong alkaline solution has had more attention paid to it (Karbhari and Abanilla, 2007).

To date, a number of research works have been conducted on the durability of various FRPs in a range of environmental conditions, such as humidity, immersion in various solutions, temperatures, and static or dynamic stresses (Karbhari and Xian, 2009; Xian and Karbhari, 2007b). Most durability studies have been focused on a single environment, which is obviously apart from the real situations of FRPs in practice. FRPs applied in strengthening civil engineering structures, in many cases (such as concrete beam strengthening), have to face the combined effects of sustained stress and various environments of immersion, temperatures and etc. The combined effects on the long-term performance of FRPs as well as FRP strengthened structures have already been considered as a critical topic for the application FRPs in civil engineering (Almusallam and Al-Salloum, 2006; Helbling and Karbhari, 2008; Laoubi et al., 2006; Love et al., 2007).

By now, a few researchers have already conducted durability work of FRPs under combined stress/strain together with various environments. Helbling and Karbhari (2008) studied water sorption and the tensile performance of a unidirectional pultruded E-glass/vinylester composite subjected to synergistic hygrothermal exposure and sustained bending. The sustained strain showed an accelerative effect on both water uptake and the degradation of tensile performance. The matrix cracking and fiber-matrix debonding were attributed to higher water uptake as well as the degradation in tensile strength. The sustained strain around 35.9% showed a transition in degradative response of a GFRP composite. The effect of tap water and sea water immersion on the long-term behavior of GFRP bars in concrete beams subjected to sustained loads were also reported, and a significant loss in strength was found (Almusallam and Al-Salloum, 2006). Laoubi et al. (2006) studied the effect of freeze-thaw cycling and sustained bending on GFRP strengthened concrete beams, and found that no obvious degradation occurred on the beams.

In this chapter, the durability of a UV curable GFRP composite (UV-GFRP) developed for fast repair of concrete structures is reported when it is subjected to a water or alkaline solution. The effect of sustained bending is also presented on the degradation of the UV-GFRP during immersion.

## 4.2 Raw materials and testing methods

The studied UV-curable resin system, developed in the Lab for FRP Composite and Structure (Harbin Institute of Technology, China), is a mixture of Bisphenol A epoxy acrylate, polyester acrylate and diluent of TPGDA ( $\text{CH}_2=\text{CHO}(\text{OC}_3\text{H}_6)_3\text{OCOCH}=\text{CH}_2$ ) monomer. The photoinitiator is 2-hydroxy-2-methylpropiophenone, bought from CAC Group Co., Ltd of China. The viscosity of the resin with 2 wt.% initiator at 25°C is

about 4000 mPa.S. Unidirectional glass fabric was kindly offered by Fyfe Co. (San Diego, USA,) with the brand name of SEH 51A.

A UV lamp was bought from Xinlan Electric Light Source Co, Ltd (Henan, China) to cure the UV systems. The UV lamp gives UV light with the wavelength of 365 nm, 1000 W, and the UV intensity is 80W/cm<sup>2</sup>.

UV curable resins with 2 wt.% of photo-initiator were mixed by hand for at least five minutes. The mixture was then used to saturate a layer of glass fabric with a hand layup process, and then cured with the UV lamp. With the UV lamp, the saturated layer of glass fabric can be fully cured in 25 s, and the resulted glass transition temperature is 58°C, and the tensile strength, modulus and strain at break are 484 MPa, 27.1 GPa and 1.94%, respectively. The nominal thickness of the fabricated GFRP plate is set as 1.3 mm, and the fiber content is 47.9 wt.% measured with the burn off testing method. Note, the tensile properties of the cured UV-GFRP composites are comparable to the epoxy based GFRP plates, which is shown in the datasheet of glass fiber fabric by the manufacturer.

The cured UV-GFRP sample coupons were cut into strips in fiber direction with the dimensions of 250 mm x 10 mm x 1.3 mm for tensile testing. For the samples tested under sustained bending deformation, metal fixtures were set up to impose the strip of bending deformation, according to the three-point bending testing fixture (Xian et al., 2013). The imposed strain was adjusted with the position of the middle rod, made of stainless steel. Two strain levels were adopted. One was 25% of its ultimate strain (0.485%) and the other was 40% of its ultimate strain (0.776%).

Samples (with or without bending) were immersed in distilled water or in alkaline solution (simulated concrete pore water with pH value of 12.5) at various temperatures (for samples subjected to bending only room temperature used). The alkaline solution was made according to ACI440 3R-04 (Guide test methods for fiber-reinforced polymers (FRPs) for reinforcing or strengthening concrete structures). The alkaline solution consists of 118.5 g of Ca(OH)<sub>2</sub>, 0.9 g of NaOH, and 4.2 g of KOH per 1 liter of distilled water.

The tensile properties of the unidirectional UV-GFRPs were tested according to ASTM D 3039 with a tensile speed of 5 mm/min. For each condition, five samples were repeated and the average results were reported.

Aged UV-GFRP samples (50 x 10 x 1.3 mm<sup>3</sup>) cut from the middle part of the aged sample in fiber direction were used for a DMTA (Dynamic mechanical thermal analysis) test at a frequency of 1Hz, a strain of 0.025% and a heating rate of 5°C from 25 to 160°C in three point bending mode using an EXSTAR DMS6100 dynamic mechanical thermal analyzer (produced by SII NanoTechnology Inc, Japan).

### 4.3 Thermal aging of UV-GFRP without sustained bending

#### 4.3.1 Water diffusion and uptake in UV-GFRP coupons

For the water uptake curves of UV-GFRP coupons at room temperature (i.e., 20°C), the initial weight gain of the samples increases linearly as a function of the square root of time, followed by leveling off of water uptake (Figure 4.1). This characteristic indicates that the water diffusion process is following Fick's law (Chin et al., 1997). At elevated temperatures (i.e., 40 and 60°C), however, a dramatic mass loss was found for the coupons immersed in both water (Figure 4.1a) and alkaline solution (Figure 4.1b). Much more mass loss was occurred for the coupons immersed in alkaline solution and/or at higher temperatures. The mass loss of the UV-cured acrylate resin system was attributed to the leaching of un-reacted monomers and small molecules (Aithal and Aminabhavi, 1990; Tey et al., 2007), and decomposition of acrylate bonding, especially catalyzed by alkaline ions at high temperatures.

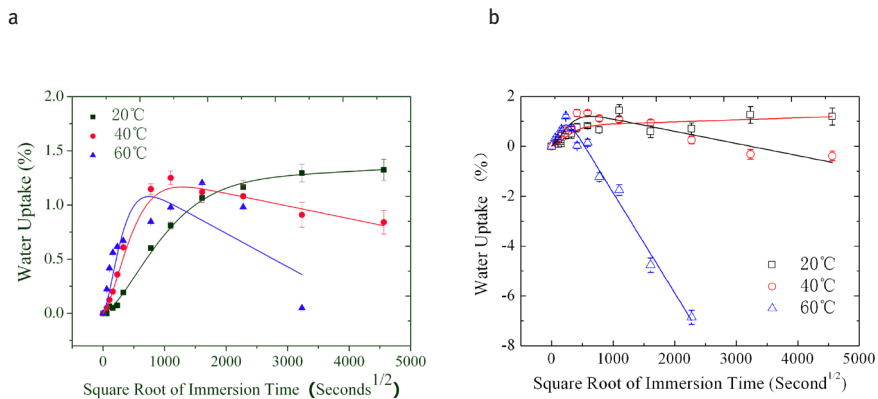


**Figure 4.1:** Water uptake of 40mm UV-GFRP coupons as a function of square root of immersion time for water immersion (a) and alkaline solution immersion (b). (Xian et al., 2012)

Due to the severe mass loss, Fick's law cannot be used to determine the diffusivity and saturate water content of the present UV-GFRP composite at higher temperatures (Crank, 1975; Xian and Karbhari, 2007b). In view of this, a two-stage model (Bao et al., 2001) that included the water diffusion process due to water concentration gradient (first stage) and the water diffusion due to polymer relaxation (second stage), was adjusted to describe the current case. The mass loss process was considered to represent the above second stage of weight change rather than polymer relaxation.

The equation describing the modified two-stage water diffusion model is given below (Bao et al., 2001).

$$M_t = M_\infty (1 + k\sqrt{t}) \{1 - \exp[-7.3(\frac{D_a t}{h^2})^{0.75}]\} \quad (4.1)$$

where  $M_t$  is the mass change rate at time  $t$ ,  $M_\infty$  is the quasi-equilibrium water uptake,  $D_a$  is the moisture diffusivity,  $k$  represents the constant rate of decomposition of the macromolecules as modified by (Wrosch et al., 2008) rather than polymer relaxation, and,  $h$  is the thickness of the specimen.

It is noteworthy that due to the loss of the integrity of samples at 60°C, the weight of samples was only tracked for about 2 months for the samples immersed in alkaline solution and 4 months for the samples immersed in distilled water (Figure 4.1). Solid lines in Figure 4.1 are curve fitting with Equation 1. A perfect fitting is realized, indicating the modified two-stage model can simulate the water uptake and mass loss process of the UV-GFRP systems. With the curve fitting method, water diffusion and uptake parameters ( $M_\infty$ ,  $k$  and  $D_a$ ) of the UV-GFRP coupons were determined and summarized in Table 4.1 for each case.

**Table 4.1:** Water diffusion and uptake parameters of 40mm UV-GFRP coupons (20mm in width and ~1.0mm in thickness) immersed in distilled water or alkaline solutions, determined with curve fitting. (Xian et al., 2012)

Medium	Immersion Temperature [°C]	$M_{\max}^*$ [%]	$M_\infty^{**}$ [%]	$\Delta m$ [%]	$k$ [ $10^{-5}/s^{1/2}$ ]	$D_a$ [ $10^{-7}mm^2/s$ ]
Distilled Water	20	1.32	1.30	-0.02	0	1.77
	40	0.84	1.34	0.50	-8.7	8.50
	60***	0.049	1.35	1.30	-22.8	18.42
Alkaline Solution	20	1.20	1.72	0.52	-3.23	4.42
	40	-0.38	1.80	2.18	-31.14	16.75
	60***	-6.86	2.16	9.02	-186.0	65.48

Note, \*,  $M_{\max}$  is ultimate water uptake ratio; \*\*,  $M_\infty$  determined from the curve fitting with Equation 1; \*\*\*, water uptake testing at 60°C was performed by 4 months in water and 2 months in alkaline solution.

For 40 mm UV-GFRP samples, the equilibrium water contents ( $M_\infty$ ) for water immersion, ranging from 1.30% to 1.35% is slightly dependent on the immersion temperatures (Table 4.1). For alkaline solution immersion, however,  $M_\infty$  from 1.72 ~ 2.16 is obviously higher than that in water immersion (Table 4.1). The higher value of  $M_\infty$  is assigned to the hydrolysis of the UV cured resins, which may bring in lots of holes / cavities on the surface, and debonding of fibers, leading to more spaces for water absorption. The higher the temperatures, the stronger the catalysis of the alkaline ions, the more serious hydrolysis occurred, and the more water was absorbed.

The difference between  $M_{\max}$  (the ultimate weight gain directly read from water uptake curve) and  $M_{\infty}$  is designated as  $\Delta m$  (equal to  $M_{\infty} - M_{\max}$ ) can be considered to represent the mass loss during the whole immersion period. As shown in Table 4.1,  $\Delta m$  increases with immersion temperatures monotonically for both water and alkaline solution immersion cases. Meanwhile, coupons immersed in alkaline solution exhibit much higher  $\Delta m$ .

$D_a$  of UV-GFRP coupons determined by curve fitting is also summarized in Table 4.1.  $D_a$  values increase with the immersion temperatures for both water and alkaline immersion, consistent with the previous works (Chin et al., 1997; Zhou and Lucas, 1999). Besides, the immersion medium also shows a remarkable effect on  $D_a$  as shown in Table 4.1. In the case of the alkaline solution,  $D_a$  is about 2 ~ 3 times higher than that in water. This result may be attributed to the hydrolysis of the resin and debonding of the fibers, which brings in more water diffusion paths.

According to Shen and Springer (1976),  $D_a$  for a unidirectional continuous fiber reinforced composite can be defined as follows:

$$D_a = D_x \left( 1 + \frac{h}{l} \sqrt{\frac{D_z}{D_x}} + \frac{h}{w} \sqrt{\frac{D_y}{D_x}} \right)^2 \quad (4.2)$$

where  $D_x$ ,  $D_y$  and  $D_z$  are the diffusion coefficients in the  $x$ ,  $y$  and  $z$  directions. In the present system, the  $z$  direction is defined as parallel to fibers,  $h$  is thickness of the specimens,  $w$  is width of the specimens,  $l$  is the length of the specimen.

For a unidirectional composite,  $D_x = D_y$  and then equation 2 can be rewritten in the following form (Chateauinois et al., 1994):

$$\sqrt{D_a} = \left( 1 + \frac{h}{w} \right) \sqrt{D_x} + \frac{h}{l} \sqrt{D_z} \quad (4.3)$$

Thus, a plot of  $\sqrt{D_a}$  versus  $h/l$  should yield a straight line with a slope  $D_z$  and an interception  $(1 + \frac{h}{w})\sqrt{D_x}$ . Based on this method,  $D_x$  and  $D_z$  were determined except for the coupons immersed in alkaline solution at the temperatures at elevated temperatures (40 and 60°C). At elevated temperatures, the coupon immersed in the alkaline solution lost their integration due to serious hydrolysis of the resin and none of linearity of  $\sqrt{D_a}$  versus  $h/l$  exists.

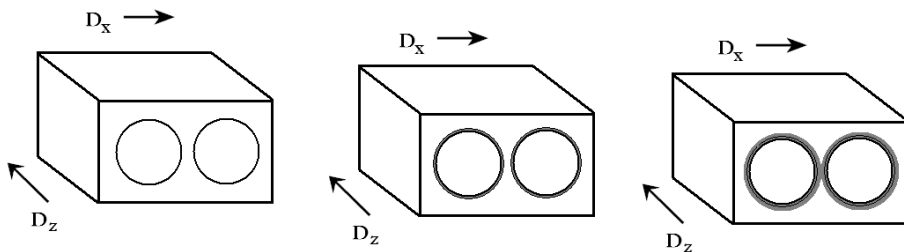
Table 4.2 presents  $D_x$ ,  $D_z$  and  $D_z/D_x$  for the UV-GFRP coupons, respectively. As shown, for the case of distilled water,  $D_z$  are much higher than  $D_x$ , indicating that water more easily diffused into the coupons along fibers. With the increase of the immersion temperature, the ratio of  $D_z/D_x$  dramatically increases from 6.4 at 20°C to more than 62.5 at 60°C. This is attributed to the debonding of the fibers from the resin at such high temperatures, which brings in more diffusion paths. The debonding of the fibers from the resin matrix can be indicated by the fractograph of immersed UV-GFRP samples, where very few resins were attached to the fibers after immersion in water and alkaline at 60°C for 4 months. The sizing of the glass fiber fabrics, which is specially designed for epoxy resins, may not form a good bonding with the current UV cured resin system and is more vulnerable to the attack from water or alkaline ions (Xian et al., 2012).

**Table 4.2:**  $D_x$ ,  $D_z$  and  $D_z/D_x$  values for UV -GFRP coupons determined experimentally. (Xian et al., 2013)

Medium	Immersion Temperature [°C]	$D_x$ [ $10^{-7}$ mm <sup>2</sup> /s]	$D_z$ [ $10^{-7}$ mm <sup>2</sup> /s]	$D_z/D_x$
Distilled Water	20	1.21	7.72	6.4
	40	3.83	260	67.9
	60	9.36	585	62.5
Alkaline Solution	20	3.0	79.5	26.5

It is worthy noting that the ratio of  $D_z/D_x$  adversely decreased very slightly as the temperature increased from 40 to 60°C (Table 4.2). This can be understood that the debonding of fiber and resin further expanded at 60°C, which leads to more diffusion paths perpendicular to the fibers. The mechanisms of water diffusion can be illustrated in Figure 4.3. At room temperature in distilled water, the interface between fiber and resin is intact,  $D_x$  is less than  $D_z$  mainly due to the block effect of fibers (Figure 4.3a). At higher temperatures (e.g. 40°C), debonding between fiber and resin occurred (Figure 4.3b), leading to much higher  $D_z$ . Further increasing the immersion temperature, the craze due to debonding expanded and connected each other (Figure 4.3c), bringing in additional diffusion path perpendicular to fibre direction.  $D_x$  thus increases comparably. The ratio of  $D_z/D_x$  will not continuously increase with the immersion temperatures.

Table 4.2 also presents  $D_x$ ,  $D_z$  and the ratio of  $D_z/D_x$  for immersion in alkaline solution at 20°C. It is interesting to compare those parameters for water immersion at the same temperature. As found,  $D_x$ ,  $D_z$  and the ratio of  $D_z/D_x$  for alkaline solution all much higher than those for distilled water. As expected, the UV-cured acrylate is easily decomposed by the catalyst effect of the alkaline solution. The interface between fiber and matrix may be a weak zone, and is susceptible to the alkaline solution. The resulted debonding is undoubtedly responsible for the higher coefficient of diffusion in both directions.

**Figure 4.3:** Evolution of debonding of fibers from resin matrix. a) no debonding, b) debonding, and c) debonding expanded and craze connected. (Xian et al., 2012)

In addition to the experimental methods as shown above,  $D_x$  along and perpendicular fibre directions can be estimated with some models. Along the fibre direction, if the effect of interfaces between fiber and matrix on the water diffusion is negligible,  $D_z$  is given as (Karbhari and Xian, 2009)

$$D_z = D_r(1 - v_f) \quad (4.4)$$

where  $D_r$  is the diffusivity of the resin matrix,  $v_f$  the volume content of fibers. The coefficient of diffusion ( $D_r$ ) of the pure resin was previously determined as  $3.1 \times 10^{-7}$  mm<sup>2</sup>/s at 20°C and  $37.3 \times 10^{-7}$  mm<sup>2</sup>/s at 60°C in water, and  $3.7 \times 10^{-7}$  mm<sup>2</sup>/s at 20°C,  $36.4 \times 10^{-7}$  mm<sup>2</sup>/s at 60°C in alkaline solution, respectively. Based on the analogy of thermal conductivity (Shen and Springer, 1976), the transverse diffusivity ( $D_x$ ) with a square fiber array is shown in the following:

$$D_x = D_r(1 - 2\sqrt{\frac{v_f}{\pi}}) \quad (4.5)$$

It is worth noting that such a model is successful in predicting the transverse diffusivity for a low fiber content of unidirectional fiber (e.g., ~ 50 vol.%) reinforced composites reported in the literatures (Kondo and Taki, 1982).

The calculated  $D_x$  and  $D_z$  based on Equation 4 and 5 are significantly lower than the values determined experimentally. The huge variation can be attributed to the assumption that the interface between fiber and resin will not contribute to the water diffusion. Clearly, this is inappropriate for the current UV-GFRP system.

#### 4.3.2 Variation of the glass transition temperatures

Immersion in water or alkaline solutions reduces the glass transition temperatures of the UV cured GFRP samples (see in Figure 4.4), remarkably. The higher the immersion temperatures, the more serious degradation of the glass transition temperatures. The alkaline solution brings in more serious depression of the glass transition temperatures, since the glass transition temperature is related to the chain length for a polymer, and the water plasticization effect (Xian and Karbhari, 2007b). Due to the serious decomposition of the resin system especially at high temperature and in the alkaline solution, the preceding effect, polymer chain breakage, is believed to be the main reason for the depression of glass transition temperature.

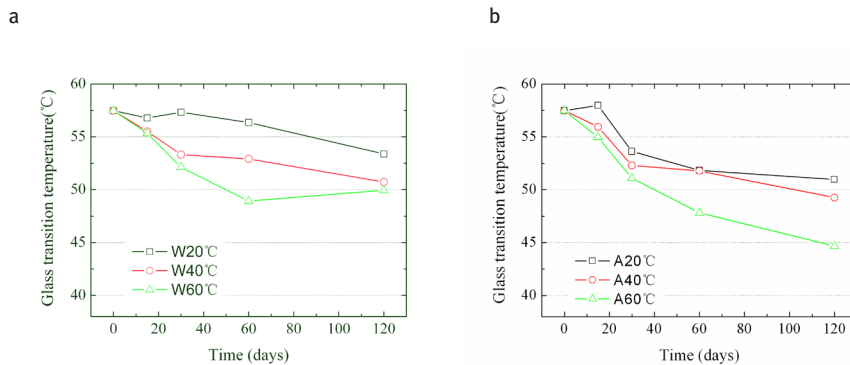


**Figure 4.4:** Evolution of glass transition temperatures of UV GFRP samples as a function of immersion time in water (a) and alkaline solutions (b) at various temperatures. (Xian et al., 2012)

### 4.3.3 Variation of the tensile properties

#### 4.3.3.1 Tensile properties of UV-GFRP immersed in water

The tensile strength, modulus as well as the elongation at break of UV-GFRP immersed in water at various temperatures steadily decreases with immersion time. The higher the immersion temperature, the more the decrease. At 40 and 60°C, the tensile strength decreased rapidly at the first two weeks. After that period, the degradation rate slowed down. However, the tensile strength at 23°C is well retained. After immersion for 3 months, the retention of tensile strength for water aged specimens is 85.7%, 72.8% and 55.6% with the temperature increasing, respectively.

Compared to the tensile strength, the modulus was less degraded by the water immersion. For 23 and 40°C water immersion, the retention of the tensile modulus was closed, about 82% after 4 months of immersion. At 60°C, the retention of the tensile modulus is 67.4%. Since the tensile modulus is more related to the stiffness of the reinforcing fibers, it is not surprising that the deterioration of the modulus is less than the strength (Svetlik, 2008).

Despite the serious degradation, UV-GFRP samples still exhibited linearity in tension. The elongation at break was also susceptible to water immersion. After 4 months of immersion, the elongation at break of the specimens immersed in 40 and 60°C water decreases from 1.9% to 1.4%. At room temperature, similar to the tensile strength, the tensile elongation was slightly affected by the water immersion.

Based on the Arrhenius equation, the service life of the UV-GFRP samples immersed in water can be estimated (Bank et al., 2003). Suppose the service temperature is the room temperature, e.g., 23°C, the predicted tensile strength retention can be determined. As found, after 50 years service at room temperature with water immersion, the tensile strength retention of UV-GFRP can reach 77.6%.

According to ACI 440.2R-02 (American Concrete Institute, Guide for the design and construction of externally bonded FRP systems for strengthening concrete structures), when a glass fiber reinforced epoxy based GFRP used exteriorly for bridge, pier as well as unenclosed parking garages, the experimental reduction factor is 0.65, while when used in an aggressive environment (such as chemical plants and waste water treatment plants), the environmental reduction factor is 0.5. Therefore, the current UV-GFRP system can be acceptable for the application of strengthening bridge, pier etc., where water immersion is inevitable.

#### **4.3.3.2 Tensile properties of UV-GFRP immersed in alkaline solution**

Compared to the water immersion, the UV-GFRP samples showed more serious degradation in tensile properties after the same immersion period. Similar to the water immersion, UV-GFRP exhibited a rapid degression in the tensile strength, especially at higher temperatures. After 4 months, the tensile strength retention is only 88%, 57% and 40% at room temperature, 40°C and 60°C, respectively. The tensile modulus is less affected by the immersion in alkaline, and the retention ratio ranges from 65% to 80% after three year immersion, which is similar to the water immersion. The elongation at break also shows remarkably temperature dependent. At 40°C and 60°C, the maximum strain reduced to around 0.8%, while the strain is around 1.8% at room temperature. The severer degradation of UV-GFRP system in alkaline solution can be attributed to the vulnerable UV-resins, which was indicated by the water uptake behaviors shown above.

According to the prediction method with the Arrhenius equation as shown above, the predicted tensile strength retention when immersed in alkaline solution can be predicted. As found, immersed in alkaline solution for only one year, the tensile strength only remains 58.1% of initial values. The fast decrease of the tensile properties suggested that the current UV-GFRP system is not suitable for the application in alkaline environments.

## **4.4 Aging of UV-GFRP under combined immersion and sustained bending at room temperature**

### **4.4.1 Water uptake and diffusion**

Water uptake curves of UV-GFRP strips immersed in water or alkaline solution under sustained bending with 0 (free sample), 25% and 40% of the ultimate strain are presented in Figure 4.5. As found, all water uptake curves follow Fick's law: the water uptake initially linearly increasing and then leveling off with square root of immersion time (Karbhari and Xian, 2009). The diffusion parameters for each case

were determined with the curve fitting method with the Fickian equation, as shown in ref. (Xian and Karbhari, 2007b):

$$D_a = \frac{\pi}{16} \left( \frac{h}{M_\infty} \right)^2 \left( \frac{dM}{dt^{1/2}} \right)^2 \tag{4.6}$$

where  $D_a$  is the apparent coefficient of diffusion,  $h$  is the thickness of the specimens,  $t$  is the exposure time and  $M_\infty$  is the saturation water uptake. The dot lines in Figure 4.2 represent the curve fitting curves with Equation 6, which are almost perfect in line with the tested data points. The determined  $M_\infty$  and  $D_a$  were summarized in Table 4.1 & 2 for both immersion cases. The rate of diffusion ( $k$ ) was calculated from  $M_\infty$  and  $D_a$ , supposing one-dimensional diffusion with the following equation (Neumann and Marom, 1987):

$$D_a = \pi(k / 4M_\infty)^2 \tag{4.7}$$

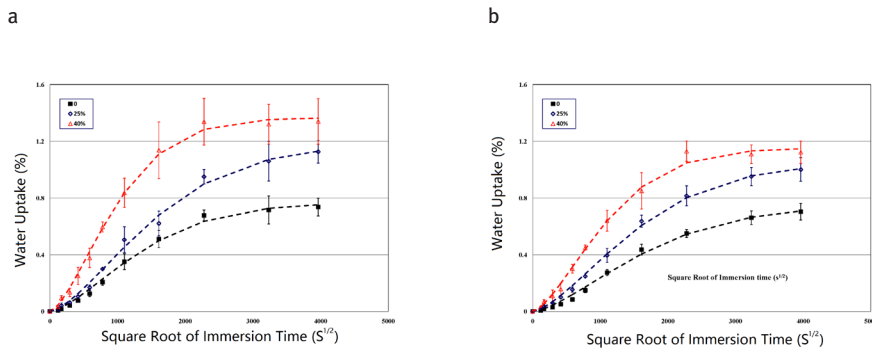


**Figure 4. 5:** Water uptake curves of the UV–GFRP specimens immersed in water (a) or alkaline solutions (b) under different bending strain at room temperature. The dot lines represent curve fitting with the Fickian model. (Xian et al., 2013)

The calculated  $k$  were also summarized in Table 4.3.

**Table 4.3:** Equilibrium water uptake ( $M_\infty$ ) and coefficient of diffusion ( $D_a$ ) for UV-GFRP specimens immersed in water. (Xian et al., 2013)

Bending strain level	$M_\infty$ (%)	$D_a$ ( $10^{-7}mm^2/s$ )	$k$ ( $10^{-6}mm/s^{1/2}$ )
0	0.77	0.49	3.85
25%	1.17	0.38	5.15
40%	1.36	0.92	9.31

As shown in Table 4.3, the imposed bending strain brings in much more water uptake, the higher the sustained bending, the higher the absorbed water content. For the rate

of diffusion, the same trend is found. Similar results were reported on a pultruded vinyl ester based GFRP composite (Helbling and Karbhari, 2008; Love et al., 2007). For the apparent coefficient of diffusion ( $D_a$ ) in both cases of immersion, however, there is no such monotonic trend. A very slight change in  $D_a$  was occurred when the sustained bending increased from 0 to 25%, while a dramatic increase in  $D_a$  was realized as the sustained bending continuously increased by 40%. The variation of the water uptake parameters was attributed to the change of water absorption mechanisms under different sustained bending levels.

Two mechanisms of water uptake in a fiber reinforced composite were expected (Neumann and Marom, 1986; Youssef et al., 2009). One is related to the free volume of the polymer matrix, and the other is related to the defects in the composites, e.g., voids and debonding of fibers from the polymer resin (leading to the wicking effect) (Thomason, 1995). For the mechanisms with the free volume, the external tension stress will lead the free volume to increase, and thus the enhanced water diffusion coefficient and water uptake (Love et al., 2007; Neumann and Marom, 1986; Youssef et al., 2009). On the contrary, the compression decreases the volume content of the system, bringing in reduced water diffusion coefficient and water uptake. For the mechanisms with defects inside of the system, the water flow and storage in the microcracks as well as the interfaces between debonded fiber and matrix can bring in much remarkable water uptake, diffusion rate (Thomason, 1995). For the present UV-GFRP system, the ultimate strain is around 1.94%, and the imposed tensile strain on the tension side only about 0.485% to 0.776%. Therefore, the macro-cracks of the UV-GFRP will not occur for both strain levels. As observed with light microscopy, even after 4 months of immersion, no cracks were found on the tension side of the UV-GFRP samples. Accordingly, under lower bending strain level (less than 25%), the free volume change due to the fact bending strain is dominant on the water absorption. However, under high bending strain (i.e., 40%), fiber debonding and the central delamination of the sample may occur, and a new path of water diffusion and new places for water uptake were created. The wicking effect is dominant, leading to much higher water uptake and diffusion. The similar mechanisms of water absorption due to sustained bending were proposed elsewhere (Helbling and Karbhari, 2008) (Love et al., 2007).

It is noted as a point of interest that the UV-GFRPs immersed in water possess higher  $E_\infty$ ,  $D_a$  and  $k$  values than those immersed in alkaline solution under the same strain levels. This can be attributed to hydrolysis of UV-cured acrylate resin catalyzed by alkaline solution, which leads to continuous mass loss and offset the water uptake and diffusion. In one of our previous studies, the hydrolysis of the UV cured acrylate resin was reported (Wrosch et al., 2008). It is worth noting that the conventionally cured GFRP composites used for rehabilitation, upgrading of civil structures are based on an epoxy resin system. The molecular structures of the cured epoxy resin system are mainly ether bonds, which is much stable than the acrylate bonds of UV curing system during immersion. In view of this, it is not surprising that the UV-GFRP

system exhibits less durable than conventional cured GFRP composites, especially during immersion.

#### 4.4.2 Variation of the glass transition temperatures

$T_g$ s of various UV-GFRP specimens (determined by the tan delta peaks) and the height of the tan delta peaks are summarized in Figure 4.6. As found, water / alkaline immersion (samples without sustained bending) leads to a remarkable reduction in the glass transition temperatures ( $T_g$ ). Compared to control samples,  $T_g$  decreased by 6°C for samples immersed in alkaline solution and ~8°C for samples immersed in water for six months, respectively. Additional sustained bending brings in further reduction in  $T_g$  by 2~3°C. The  $T_g$  reduction is attributed to the plasticizing effect of the absorbed water. Sustained bending creates more water uptake, being responsible for the lower  $T_g$ s.

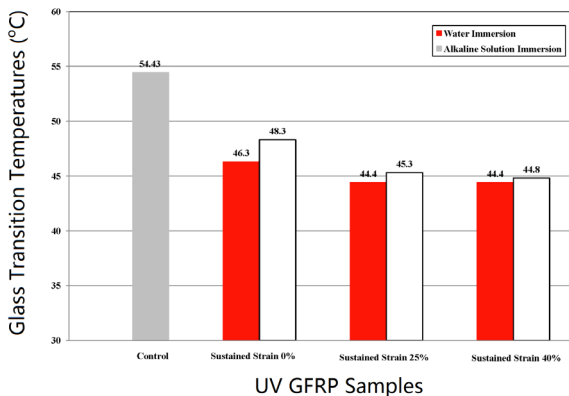


**Figure 4.6:** Glass transition temperatures of UV-GFRP samples subject to sustained strain and water /alkaline solution immersion for 6 months. (Xian et al., 2013)

Figure 4.7 shows the variation of the glass transition temperatures of UV GFRP as a function of water uptake content. As shown, the variation of  $T_g$  initially shows a reduction linearly with water content and then levels off. Note, the final data points for two curves are related to 40% bending deformation. As mentioned above, the high sustained deformation (i.e., 40% of ultimate strain) may bring in resin cracks, the debonding of fibers as well as de-lamination, which bring in extra water uptake in those defects. Only the water molecules which swell in the resin molecules and brings in more free volume (Love et al., 2007), can plasticize the resin system. Such water existing in macro-defects will not plasticize the resin. Based on this assumption, remove the final two data for the water and alkaline solution, and the effect of the

water uptake content on the depression of  $T_g$  is determined by a linearity fitting method. With 1% water uptake,  $T_g$  is reduced by 8.75°C for distilled water immersion, and 8.60°C for alkaline immersion. There is not much difference in the two cases.

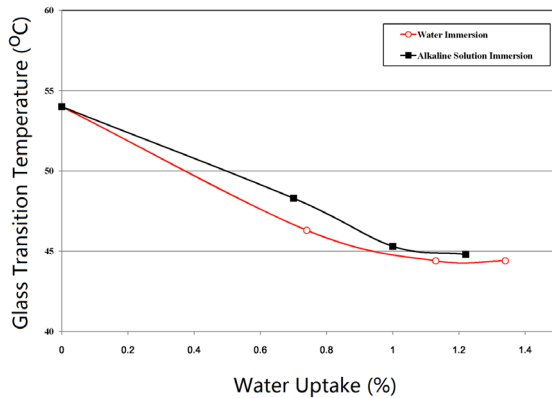


**Figure 4.7:** variation of glass transition of UV GFRP under combined effect of sustained bending and water/alkaline solution immersion for six months as a function of the content of water uptake. (Xian et al., 2013)

#### 4.4.3 Variation of the tensile properties

In ambient conditions, the tensile strength gradually reduces by 7.9% and 16.9% with sustained bending strain of 25% and 40% in 6 months. While in distilled water, more degradation in the tensile strength is found. The reduction is about 9.6% for the sustained bending strain of 25%, and 26.2% for the sustained bending strain of 40%. Clearly, combined with water immersion, the sustained strain exhibits a more detrimental effect on the degradation of the tensile strength. Compared to the water immersion, the alkaline solution immersion accelerates degradation in the strength of the UV-GFRP samples under sustained bending, significantly. In six months, the tensile strength readily decreased by 41% under 25% of bending strain, and by 48.7% under 40% of bending strain when UV-GFRPs were immersed in alkaline solution. It is worth noting that the reduction in the tensile strength of a glass fiber reinforced vinyl ester pultruded strips is around 20~26% under the similar bending conditions for a similar water immersion (Love et al., 2007).

As found, the ultimate strain gradually decreases with the aging time by 13~17%, and immersion in water does not bring more degradation. The higher the sustained bending strain leads to the higher reduction in the ultimate strain. More severe degradations of the ultimate strain were found for the combined effect of sustained

bending and alkaline solutions. This trend is consistent with the change of the tensile strength.

As mentioned in the section on water absorption, the combined effects of sustained bending and immersion may bring in fiber debonding, cracks in the resin as well as delamination, which undoubtedly can cause premature breaks of UV-GFRPs during tension, resulting in decreased the tensile strength and ultimate strain. Since alkaline immersion additionally leads to hydrolysis of the resin, more severe degradations in the strength and ultimate strain were realized.

As opposed to the tensile strength and the ultimate elongation, the tensile modulus was increased by 12% for the samples under sustained bending in ambient conditions regardless of the level of the sustained strain. Combined with the water immersion, the tensile modulus is enhanced to a similar extent for the lower sustained bending. However, under the higher sustained bending combined with distilled water, the tensile modulus exhibits much less affected. Similarly, UV-GFRPs subjected to combined sustained bending and alkaline solution exhibit clearly increases in the tensile modulus, even under a high sustained bending level. The orientation of the resins due to the sustained tension strain on the tension side of the UV-GFRP samples, as expected, can contribute to the enhanced modulus. In addition, due to the extraction of un-cured small molecules during immersion, the resin system will harden. This will also lead to the increase of the modulus.

## 4.5 Conclusions

Hygrothermal aging of UV cured GFRP composites for fast repair of concrete structures, were presented in this chapter when subjected to water or alkaline solution immersion. When immersed in water or alkaline solution without externally strain, the mass loss of UV-GFRP was found due to the decomposition of the resin; an alkaline solution and high temperatures (by 60°C) create a serious decomposition of the system. The coefficient of diffusion of water in fiber directions, determined through testing samples of various lengths, is much higher than the predicted values, due to fiber debonding especially in an alkaline solution. Tensile strength and elongation at the break of UV-GFRP samples degraded significantly, while the tensile modulus was less affected. With the Arrhenius equation, the long term evolution of tensile strength is predicted. As shown, UV GFRP can work well in a water immersion case, where the tensile strength retention at room temperature is estimated to be 77.6% of its initial values. In an alkaline solution, the tensile strength of the UV-GFRP was dramatically decreased even at room temperature and is not suitable for the application in alkaline environments.

Combined water / alkaline immersion and sustained bending brings in more degradation of a UV cured GFRP composite. As found, sustained bending accelerates the diffusion rate and increases the water uptake remarkably, the higher the bending

strain, the more water absorbed and the higher the diffusion rate. Under combined alkaline solution immersion and sustained bending, the tensile strength of the UV-GFRP decreased remarkably with aging time and sustained bending levels, while the tensile modulus increased slightly. For the case of water immersion, a similar trend was found but to a much lower extent. 1% water uptake brings in  $T_g$  reduction by  $\sim 8.6$  to  $8.75^\circ\text{C}$ .

**Acknowledgement:** This work is financially supported by NSFC with Grant No. 51478145, the National Key Basic Research Programme of China (973 Programme) with Grant No. 2012CB026200, Program for New Century Excellent Talents in University with Grant No. NCET-10-0065, and Specialized Research Fund for the Doctoral Program of Higher Education (SRFDP) with Grant No. 20102302120068.

## References

- Aithal, J.S., and Aminabhavi, T.M. (1990). Sorption And Diffusion Of Organic-Solvents In Polyurethane Elastomers. *Polymer* 31, 1757-1762.
- Almusallam, T.H., and Al-Salloum, Y.A. (2006). Durability of GFRP rebars in concrete beams under sustained loads at severe environments. *Journal Of Composite Materials* 40, 623-637.
- Bank, L.C., Gentry, T.R., Thompson, B.P., and Russell, J.S. (2003). A model specification for FRP composites for civil engineering structures. *Construction and Building Materials* 17, 405-437.
- Bank, L.C., Oliva, M.G., Bae, H.-U., Barker, J.W., and Yoo, S.-W. (2007). Pultruded FRP plank as formwork and reinforcement for concrete members. *Advances in Structural Engineering* 10, 525-535.
- Bao, L.R., Yee, A.F., and Lee, C.Y.C. (2001). Moisture absorption and hygrothermal aging in a bismaleimide resin. *Polymer* 42, 7327-7333.
- Chateauminois, A., Vincent, L., Chabert, B., and Soulier, J.P. (1994). Study Of The Interfacial Degradation Of A Glass Epoxy Composite During Hygrothermal Aging Using Water Diffusion Measurements And Dynamic-Mechanical Thermal-Analysis. *Polymer* 35, 4766-4779.
- Chin, J.W., Nguyen, T., and Aouadi, K. (1997). Effects of environmental exposure on fiber-reinforced plastic (FRP) materials used in construction. *Journal Of Composites Technology & Research* 19, 205-213.
- Compston, P., Schiemer, J., and Cvetanovska, A. (2008). Mechanical properties and styrene emission levels of a UV-cured glass-fibre/vinylester composite. *Composite Structures* 86, 22-26.
- Crank, J. (1975). *The Mathematics of Diffusion*, Clarendon Press, Oxford, 2nd edition.
- Di Pietro, A., and Compston, P. (2009). Resin hardness and interlaminar shear strength of a glass-fibre/vinylester composite cured with high intensity ultraviolet (UV) light. *Journal Of Materials Science* 44, 4188-4190.
- Duan, Y.G., Wang, Y.J., Tang, Y.P., Li, D.C., and Lu, B.H. (2011). Fabrication and mechanical properties of UV-curable glass fiber-reinforced polymer-matrix composite. *Journal Of Composite Materials* 45, 565-572.
- Helbling, C.S., and Karbhari, V.M. (2008). Investigation of the sorption and tensile response of pultruded E-glass/vinylester composites subjected to hygrothermal exposure and sustained strain. *Journal Of Reinforced Plastics And Composites* 27, 613-638.

- Hollaway, L.C. (2009). A review of the present and future utilisation of FRP composites in the civil infrastructure with reference to their important in-service properties. *Construction And Building Materials* 24, 2419-2445.
- Jumaat, M.Z., Rahman, M.M., and Alam, M.A. (2010). Flexural strengthening of RC continuous T beam using CFRP laminate: A review. *International Journal Of The Physical Sciences* 5, 619-625.
- Karbhari, V.M., and Abanilla, M.A. (2007). Design factors, reliability, and durability prediction of wet layup carbon/epoxy used in external strengthening. *Composites Part B-Engineering* 38, 10-23.
- Karbhari, V.M., Chin, J.W., Hunston, D., Benmokrane, B., Juska, T., Morgan, R., Lesko, J.J., Sorathia, U., and Reynaud, D. (2003). Durability gap analysis for fiber-reinforced polymer composites in civil infrastructure. *Journal Of Composites For Construction* 7, 238-247.
- Karbhari, V.M., and Xian, G.J. (2009). Hygrothermal effects on high V-F pultruded unidirectional carbon/epoxy composites: Moisture uptake. *Composites Part B-Engineering* 40, 41-49.
- Kondo, K., and Taki, T. (1982). Moisture Diffusivity Of Unidirectional Composites. *Journal Of Composite Materials* 16, 82-93.
- Laoubi, K., Ei-Salakawy, E., and Benmokrane, B. (2006). Creep and durability of sand-coated glass FRP bars in concrete elements under freeze/thaw cycling and sustained loads. *Cement & Concrete Composites* 28, 869-878.
- Li, G.Q., and Ghebreyesus, A. (2006). Fast repair of damaged RC beams using UV curing FRP composites. *Composite Structures* 72, 105-110.
- Li, G.Q., Hedlund, S., Pang, S.S., Alaywan, W., Eggers, J., and Abadie, C. (2003). Repair of damaged RC columns using fast curing FRP composites. *Composites Part B-Engineering* 34, 261-271.
- Love, C.T., Xian, G., and Karbhari, V.M. (2007). Thermal, mechanical, and adhesive properties of HDPE/reactive ethylene terpolymer blends. *Journal of Applied Polymer Science* 104, 331-338.
- Neumann, S., and Marom, G. (1986). Free-Volume Dependent Moisture Diffusion Under Stress In Composite-Materials. *Journal Of Materials Science* 21, 26-30.
- Neumann, S., and Marom, G. (1987). Prediction Of Moisture Diffusion Parameters In Composite-Materials Under Stress. *Journal Of Composite Materials* 21, 68-80.
- Peck, J.A., Jones, R.A., Pang, S.S., Li, G.Q., and Smith, B.H. (2007). UV-cured FRP joint thickness effect on coupled composite pipes. *Composite Structures* 80, 290-297.
- Pendhari, S.S., Kant, T., and Desai, Y.M. (2008). Application of polymer composites in civil construction: A general review. *Composite Structures* 84, 114-124.
- Shen, C.H., and Springer, G.S. (1976). Moisture Absorption And Desorption Of Composite-Materials. *Journal Of Composite Materials* 10, 2-20.
- Svetlik, S.L. (2008). An Investigation in the Hygrothermal Degradation of an E-glass/vinyl-ester Composite in Humid and Immersion Environments. PhD Dissertation, Department of Structural Engineering, University of California, San Diego.
- Tey, J.N., Soutar, A.M., Priyadarshi, A., Mhaisalkar, S.G., and Hew, K.M. (2007). Ink and moisture sorption study in UV-curable polyurethane acrylate. *Journal Of Applied Polymer Science* 103, 1985-1991.
- Thomason, J.L. (1995). The Interface Region In Glass-Fiber-Reinforced Epoxy-Resin Composites .2. Water-Absorption, Voids And The Interface. *Composites* 26, 477-485.
- Wrosch, M., Xian, G.J., and Karbhari, V.M. (2008). Moisture absorption and Desorption in a UV cured urethane acrylate adhesive based on radiation source. *Journal Of Applied Polymer Science* 107, 3654-3662.
- Xian, G., and Karbhari, V.M. (2007a). Segmental relaxation of water-aged ambient cured epoxy. *Polymer Degradation And Stability* 92, 1650-1659.
- Xian, G., Li, H., and Su, X. (2012). Water absorption and hygrothermal ageing of ultraviolet cured glass-fiber reinforced acrylate composites. *Polymer Composites* 33, 1120-1128.

- Xian, G., Li, H., and Su, X. (2013). Effects of immersion and sustained bending on water absorption and thermomechanical properties of ultraviolet cured glass fiber-reinforced acrylate polymer composites. *Journal of Composite Materials* 47, 2275-2285.
- Xian, G.J., and Karbhari, V.M. (2007b). DMTA based investigation of hygrothermal ageing of an epoxy system used in rehabilitation. *Journal Of Applied Polymer Science* 104, 1084-1094.
- Youssef, G., Freour, S., and Jacquemin, F. (2009). Stress-dependent Moisture Diffusion in Composite Materials. *Journal Of Composite Materials* 43, 1621-1637.
- Zhou, J.M., and Lucas, J.P. (1999). Hygrothermal effects of epoxy resin. Part I: the nature of water in epoxy. *Polymer* 40, 5505-5512.